# FRACTURE INTERFACE ELEMENTS FOR STATIC AND FATIGUE ANALYSIS

**Gerald E. Mabson*, Lyle R. Deobald*, Bernhard Dopker*, D.M. Hoyt**, Jeffrey S. Baylor**, Douglas L. Graesser****

***The Boeing Company, ****NSE Composites**

**Keywords**: *fracture, fatigue, finite elements, interface elements*

***Abstract***

*Fracture interface elements have been developed that enable the practical application of the virtual crack closure technique within finite element models along predetermined interfaces. These elements are especially useful if non linear behavior occurs in the model, or if crack propagation predictions are desired. This paper presents the development and application of these elements to both static and fatigue analysis.*

## 1 Introduction

Delamination can be simulated by releasing coincident nodes and making use of the well established virtual crack closure technique (VCCT) [1]. The crack tip energy release rates can be determined from finite element models with arbitrary (but non-zero) loading. These crack tip energy release rates can be easily scaled to the critical energy release rate if the model is linear. The appropriate nodes, along a predetermined crack plane, can be released or model geometry updated and the crack can be successfully propagated for single 1-D cracks with single crack tips. The fracture mechanics scaling procedure normally occurs outside of the finite element code. If multiple crack tips exist, multiple computer runs are required to propagate the cracks. Each of these runs corresponds to a different crack length. This technique requires tedious postprocessing of multiple finite element solutions. If non-linear behavior(s) exists in the model, difficulties arise in determining the load at which the crack tip energy release rate equals its critical value. Therefore, many consider this method only generally applicable to linear problems with single crack tips. This approach is not practical for addressing problems containing, multiple crack tips on one dimensional (1-D) cracks (either two tips on a single crack, or multiple cracks with multiple crack tips), or multiple finite area cracks. A description of the implementation of this technique is given in [2].

A set of finite elements have been developed that take advantage of the linear elastic fracture mechanics theory and combines it with the ease of use of interface based finite element methods [3 through 9]. These elements allow the initiation of propagation and the propagation of interlaminar cracks, disbonds or delaminations to be simulated in layered materials using fracture mechanics procedures without many separate analyses. One must only define the critical energy release rate(s), which is mesh independent. Unlike decohesive type interface element formulations, mesh dependent maximum stress levels do not need to be identified. The fracture elements are based on the mixed-mode modified virtual crack closure technique, utilize common mixed-mode delamination growth, fatigue crack onset and fatigue crack growth criteria.

## 2 Two Dimensional (2D) Fracture Element

### 2.1 General Considerations

For planar conditions, 2D fracture interface elements for mixed mode analysis of layered materials are placed at the crack plane in a finite element model. For planar problems (2D) the element is shown in Figure 1.

In the undeformed condition, nodes 1 and 6, nodes 2 and 5, and nodes 3 and 4 are coincident. The stiffnesses between all nodes of the element are zero except between nodes 2 and 5. Prior to crack propagation the stiffness between nodes 2 and 5 is infinite in all directions. The “infinite” stiffness can be modeled as a very large but finite value.

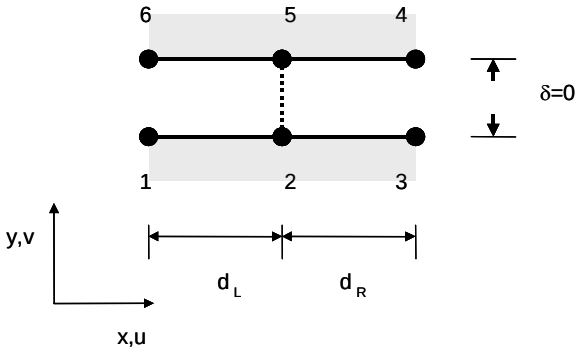


Fig. 1. Undeformed 2D Interface Element

## 2.2 Mode I

Consider a crack approaching from the left under pure mode I conditions, such that the crack tip is at nodes 2,5 as shown in Figure 2. Under self similar conditions, one can compute the energy release rate for mode I, $G_I$, available for a crack to extend from nodes 2,5 to nodes 3,4 using the following equation because force the $F_{v,2,5}$ and displacement $v_{1,6}$ are known quantities [1].

$$\frac{1}{2}\frac{v_{1,6}F_{v,2,5}}{bd_L} = G_{IC}$$

where

$G_{IC}$ = Critical mode I energy release rate

$b$ = width

$F_{v,2,5}$ = Vertical force between nodes 2 and 5

$v_{1,6}$ = Vertical displacement between nodes 1 and 6

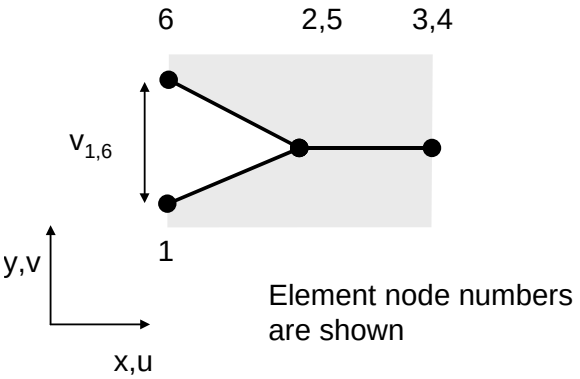


Fig. 2. Deformed 2D interface element prior to start of node release

Ideally the length $d_L$ equals the length $d_R$, however the above equation corrects for slightly different lengths $d_L$ and $d_R$. The needed displacement, $v$, is $d_R$ to the left of nodes 2,5 for the situation shown in Figure 2. Depending on the local loading and mesh size, this displacement can be approximated using various interpolation schemes. The equation above assumes that the displacement, $v$, is directly proportional to the distance to the left of nodes 2,5.

The actual energy release rate with the given load on the structure can be compared to the critical energy release rate. Nodes 2 and 5 will start to release when the computed energy release rate is larger than the critical energy release rate. Now that $F_{v,2,5crit}$ and $v_{2,5crit}$ are known, the force between nodes 2 and 5 may be incrementally released so that the area under the release curve is based on $G_{IC}$ (See Figure 3). Note that due to the assumption of self similar crack propagation, $v_{1,6crit}$ and $v_{2,5crit}$ are assumed to be equal when $d_L$ equals $d_R$. For pure mode I conditions only tensile loads cause node release.

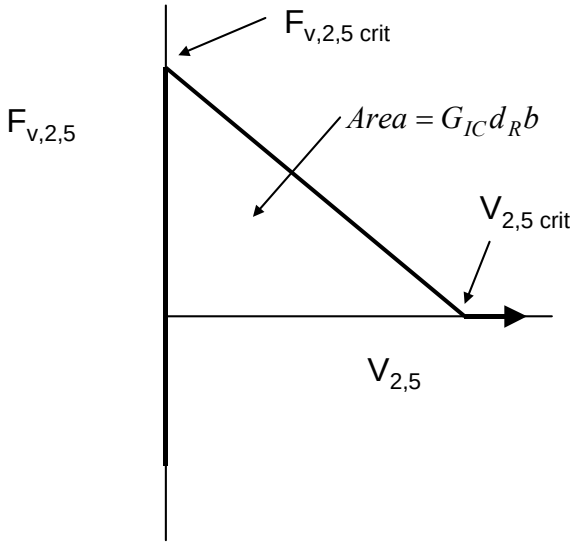


Fig. 3. Vertical load-displacement relationship between nodes 2 and 5

If the structure is unloaded after some initial fracture has occurred, the load-displacement relationship may not follow the original force-displacement relationship. Instead a reduced stiffness must be used which is a function of the amount of crack extension that has occurred. Figure 4 illustrates the proper force-displacement relationship.

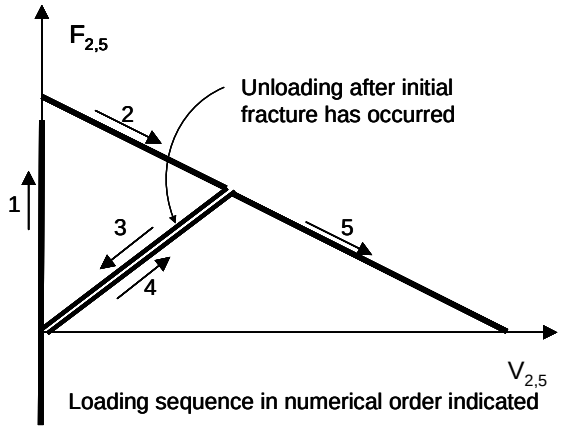


Fig. 4. Vertical load-displacement relationship between nodes accounting for unloading

## 2.3 Mode II

Pure mode II conditions are handled similarly except that the displacements and loads are measured horizontally instead of vertically, $G_{IIC}$ is used instead of $G_{IC}$, and load and displacements are tolerated in either direction. The equations used are shown below.

$$\frac{1}{2}\frac{u_{1,6}F_{h,2,5}}{bd_L} = G_{IIC}$$

where

$G_{IIC}$ = Critical mode II energy release rate

$b$ = width

$F_{h,2,5}$ = Horizontal force between nodes 2 and 5

$u_{1,6}$ = Horizontal displacement between nodes 1 and 6

## 2.4 Mixed Mode Analysis

Mixed mode fracture conditions can be modeled easily using a relationship such as

$$\left(\frac{G_I}{G_{IC}}\right)^m + \left(\frac{G_{II}}{G_{IIC}}\right)^n \geq 1, \text{ for crack propagation}$$

where

$m$, $n$, are input parameters controlling interaction

$$G_I = \frac{1}{2}\frac{v_{1,6}F_{v,2,5}}{d_L b}$$

$$G_{II} = \frac{1}{2}\frac{u_{1,6}F_{h,2,5}}{d_L b}$$

$G_{IC}$, $G_{IIC}$ are critical energy release rates for mode I and II respectively

If a crack approaches from the right (rather than the left) displacements of the right set of nodes ($u_{3,4}$ and $v_{3,4}$) and the opposite side distances are used instead of the values shown above.

The inputs required for an element are the typical element input data such as node numbers, locations for each node and the element connectivities. Note that the thickness of the element is assumed to be zero and one must provide only $G_{IC}$, $G_{IIC}$, $m$, $n$, and $b$ as element properties.

## 2.5 Crack Propagation

To model crack propagation, a series of these interface elements must be used as shown in Figure 5. By overlapping a series of interface elements, a crack can be propagated along the entire interface in either direction. The direction of crack propagation does not need to be predetermined and set as a condition in the model.

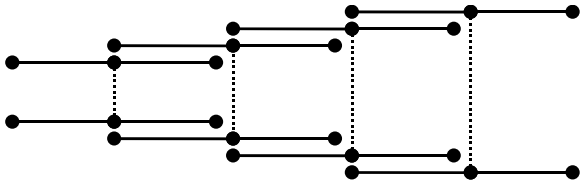

Fig. 5. Overlapping series of interface elements

## 2.6 Non-Symmetric Multi-Delamination Analysis

An example showing the capability of the element with multiple delaminations and multiple crack growth areas is shown in this section. The test data for the example was provided in [10]. The material data is as follows:

$E_{11} = 115.0\ GPa$

$E_{22} = 8.5\ GPa$

$E_{33} = 8.5\ GPa$

$G_{12} = 4.5\ GPa$

$\mu_{12} = 0.29$

$\mu_{13} = 0.29$

$\mu_{23} = 0.3$

$G_{IC} = 0.33\ N/mm$

$G_{IIC} = 0.80\ N/mm$

$a_1 = a_2 = 40\ mm$

$width = 20\ mm$

$L = 100\ mm$

Layer thickness $= 0.1325\ mm$

The geometry of the problem is shown in Figure 6.

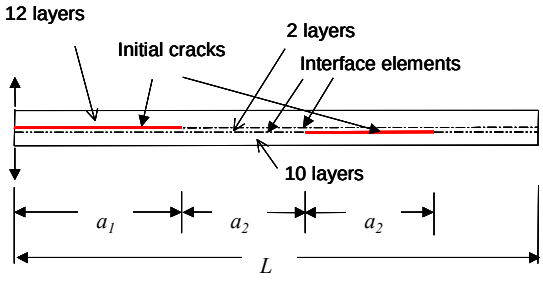


Fig. 6. Geometry of multiple delamination analysis

The results of the analysis are shown in Figure 7.

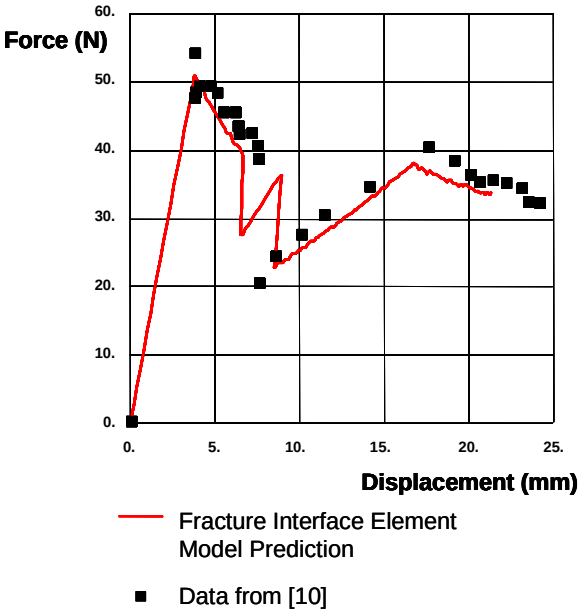


Fig. 7. Results comparison of multiple delamination analysis

This validation example is particularly difficult as it involves tracking three crack tips simultaneously and includes two unstable crack propagations. The interface elements provided a remarkably good comparison to the test results. Note that these results were obtained in a single nonlinear ABAQUS® run [11].

## 3 Three Dimensional (3D) Fracture Element

The 3D fracture interface element can model crack fronts. Figure 8 represents the 3D fracture interface element. The center nodes are initially constrained together and the four mid-side node pairs act as antennae to sense the angle of an approaching crack front. The remaining corner node pair locations are necessary to account for the element area in the energy calculations. The element senses an approaching crack front by the onset of a relative displacement between the nodes of one or more of the antennae node pairs. Once the element becomes active, the constraining forces between the center node pair and the periphery crack opening displacements are used in a fracture mechanics based failure criteria that uses $G_{IC}$, $G_{IIC}$ and $G_{IIIC}$ to determine if the center node should begin to release. Once the failure criteria is satisfied, the residual forces between the center node pair will release following a strain softening law such that the area under the force-displacement curve satisfies the fracture mechanics failure criteria. Elements are overlapped in both directions.

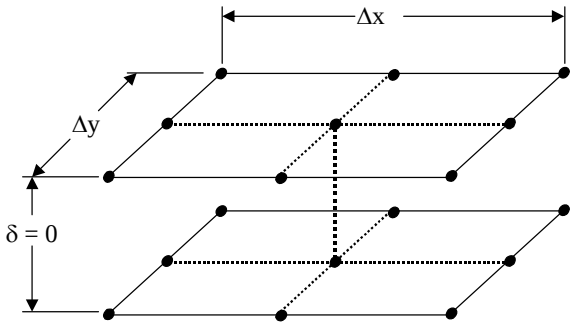


Fig. 8. 3D fracture interface element.

The static fracture interface element algorithms were coded and incorporated as user elements within the ABAQUS® general-purpose finite element framework for use by the element developers within Boeing [11]. Recently ABAQUS® has offered a similar capability that enables the wide distribution and maintenance of this technology.

## 4 Accuracy Issues with Static Fracture Elements

Accuracy of these VCCT-based interface fracture elements may be considered in terms of predicting either onset of delamination growth or propagation. Much of the discussion in the literature with regards to accuracy of the VCCT is applicable to these elements. The recommendation is made that analysts perform mesh sensitivity studies using different types of elements (for example ABAQUS® element types SC8R, C3D8, C3D8I, etc.). If 3D solid elements are selected, the suppression of the oscillating singularity may be achieved by adjusting the transverse Poisson's ratio to a value that causes Dundurs parameter, $\beta$, to be zero. Another practical issue is that of time step uncertainty. Given a chosen time step in the analysis, the critical load

level at which the delamination begins to grow will generally fall between discrete analysis loads. Linearity may be used to estimate the true value. The most significant accuracy issue associated with a 3D analysis concerns the true local growth of the crack front. Consider the double cantilever beam (DCB) test as an example. The crack is expected to grow first mid-way across the coupon and then later the crack front will become active across the entire width at a higher load. This higher load, associated with self-similar crack growth, would be more representative of the measured critical load in a DCB test, yet the analysis predicts onset of delamination at release of the very first element in the middle of the DCB. The analyst must interpret analysis results appropriately for the application. This effect is particularly acute for corner features or chevrons at the prospective plane of delamination. Crack growth from a corner feature is not self-similar and will have a relatively high apparent energy release rate. The actual tendency will be for the corner to round out before achieving self-similar growth. The load at the first release of an element at the corner may be well below the load once that corner has rounded out.

Maintaining accuracy of the analysis during the propagation phase is challenging. Once the element begins to release, a negative tangential stiffness would normally be passed back to the Newton solver. Passing the steep negative stiffness causes the solution to diverge immediately. The interface fracture element algorithms can pass a zero tangential stiffness to the solver representing a complete release of the element. More importantly, the user may select a flag to calculate a residual constraining force that precisely follows the strain softening curve or set the residual forces to zero after reaching the critical value. This second approach provides the most robust solution and affords reasonable accuracy if the time step is sufficiently large with respect to the element release time. At present, the relationship between the time for VCCT element release and the time step increment is not well understood. The ABAQUS® automatic cutback feature is suppressed when doing the propagation analysis with the interface fracture elements. In general, the elements display a trade-off between solution stability, solution time and accuracy when performing a propagation analysis. Understanding these effects has permitted successful analysis through the control of the time step and convergence tolerances in ABAQUS®. However, more investigation is needed to fully understand the interaction of the VCCT element release with the nonlinear solver.

## 5 Fatigue Fracture Elements

### 5.1 General Considerations

Interlaminar fatigue analysis has historically been tedious to perform. Two published methods for interlaminar fatigue analysis make use of the crack tip energy release rate [12, 13]. Fatigue growth may be predicted with a Paris law that relates the energy release rate ($G$) to crack growth rates (Paris law method). Another approach determines the onset of fatigue growth for a given number of load cycles at a given level of $G$ ($G_{ONSET}$ method). Both approaches assume preexisting damage in the structure and both use coupon fracture fatigue test results (e.g. DCB for mode I) to calibrate the fatigue laws. The challenge in analysis of realistic composite structure is that the structure may contain multiple crack tips or crack fronts. One must also consider a nonlinear structural response when the structure is subjected to either a constant loading at a user specified load ratio, *Pmax/Pmin*, or the structure must be evaluated for spectrum loading. In practice, impact damage may have an irregular shape that is permitted to "round-out" in determining the life of the structure in order to satisfy a "no-growth" criterion.

The 2D static fracture element has been extended to allow the prediction of fatigue performance.

The fatigue fracture element can perform both the Paris law and $G_{ONSET}$ analysis methods depending on the input syntax. The advantage of the fatigue fracture element approach, is that it can handle any number of crack tips or crack fronts. The elements may be modified to include geometric or material nonlinearity as will be described here. A typical design criterion is to not allow a delamination to grow during two lifetimes of service, however in practice, irregularly shaped delaminations may be permitted to "round-out". An analysis is needed whereby the life of the structure may be determined as a function of cyclic load levels. An extent of crack growth must be specified to define the end of the fatigue life.

### 5.2 Paris Law Fatigue Growth

For fatigue loading, composite structures are often subjected to a "no-growth" criterion. In other words, manufacturing flaws and barely visible impact damage (BVID) are not permitted to grow for two lifetimes of the structure. However, this

leads to a practical issue where irregularly shaped damage or delaminations will "round-out" when subjected to a small number of load cycles. This small amount of growth is nearly indiscernible and does not change the residual strength of the structure. A certifying organization may take the approach to permit only a small amount of detectable crack growth in the structure. This approach meets the structural requirements without severely penalizing the structure for small local growth.

The objective is to determine, that if *Pmax* and initial cracks (or crack fronts) are given, the crack growing direction (shape) and length, *a*, after "*N*" cycles. The model must be able to determine the growth rate, *da/dN*, as a function of *Pmax* or *ΔP* (for a constant R-ratio in a given load block). Experimentally, *da/dN,* for mode I, can be characterized based on or by testing DCB coupons under fatigue loading [14]. Crack growth in the Paris regime can be fitted to the following equation forms:

$$\frac{da}{dN} = C_o \cdot G_{\max}^{\beta} \quad \text{or} \quad \frac{da}{dN} = C_o \cdot (\Delta G)^{\beta}$$

$$\text{for } G > G_{thresh}$$

The Paris law is a logarithmic fit to DCB crack growth data as shown in Figure 9. The relationship is based on $G_{max}$ or $\Delta G$ where $G$ is the energy release rate to be calculated in the finite element (FE) model. In the Paris Law equations, *da/dN* is the crack growth per loading cycle, $C_o$ and $\beta$ are constants determined by fitting the DCB test data (for mode I), $\Delta G$ is the difference in energy release rates between the maximum and minimum load, $G_{max}$ is the energy release rate when the structure is loaded to its peak load (this assumes the same R-ratio in the FE models as was acquired in the DCB test data).

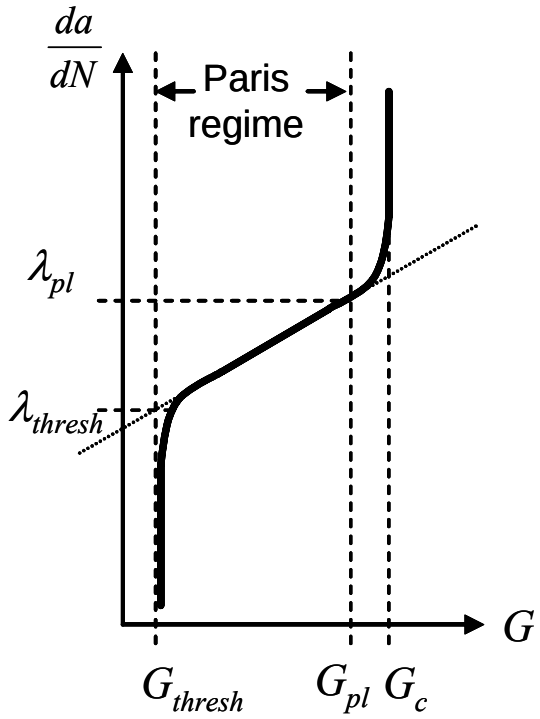


Fig. 9. Paris law fatigue growth regime

Where

$G_{Ipl}, G_{IIpl}$ = Energy release rates in mode I and II defining upper limit of the Paris regime

(Note : *pl* refers to "Paris limit")

$G_{thresh}$ = Fatigue threshold energy release rate

$\lambda_{pl}$ = Crack opening rate (*da/dN*) at the upper end of the Paris regime

$\lambda_{thresh}$ = Crack opening rate at the fatigue threshold

Separate growth equations are fitted for the various crack propagation modes. The fatigue fracture elements support both forms ($G_{max}$ and $\Delta G$) of the Paris law shown above.

Consider a problem with multiple crack tips. The application of the Paris law is shown in the flow chart in Figure 10. The fatigue fracture elements at the active crack tips will sense crack opening associated with applied loading. Given input empirical parameters $C_o$ and $\beta$, combined with the known node spacing $d_R$ and $d_L$ shown in Figure 1, the number of cycles necessary to fail each particular element may be calculated as $dn_j$. At this point, the elements within the model must communicate between one another to properly coordinate element release. The first instance of a fatigue fracture element is defined as the "Master

Element" and calculations are made within this element to perform the bookkeeping function for all active elements. A crack growth rate is calculated for all elements that have a calculated $G$ greater than a threshold value, $G_{thresh}$, and less than the Paris Limit, $G_{Paris\ Limit}$. The crack growth rate value is used to calculate the number of cycles required to fail each active fatigue element. This calculation is based on a crack length, $da$, that is the difference between the applicable element dimension, $\Delta x$ ($d_R$ for a crack traveling to the right) less any accumulated damage from prior increments. The element with the fewest number of cycles, $N_{MIN}$, remaining to failure is released completely setting constraining force at the center node pair to zero. This minimum number of cycles to failure is added to the accumulation of cycles from prior increments and this total represents the structural life to grow the crack to this particular location. Before proceeding to the next increment, each active element must accumulate damage associated with the number of cycles accumulated in the current increment. An accounting of accumulated damage is made for all remaining elements. As each element is released, the load is redistributed and a new $G$ must be calculated for each active element. The analysis is setup to release one element or more per increment in the nonlinear ABAQUS® analysis and the cumulative number of cycles is reported to the data file.

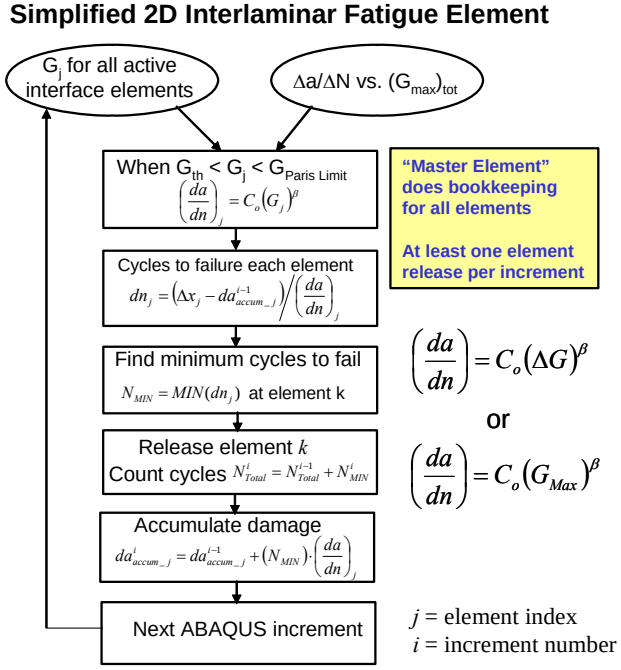


Fig. 10. Flow chart for Paris law fatigue growth analysis

Element usage is shown in Figure 5 where layers in model are constrained together with fatigue fracture elements with antennae nodes from one element overlapping the constrained node pair of the adjacent element. At least one antennae node pair must be initially unconstrained to represent the initial crack tip. Figure 11 shows the fine and coarse mesh finite element models of a DCB that were used to verify the element functionality. Figure 12 shows the ABAQUS® load step used to demonstrate the analyses in comparison with a theoretical DCB solution. Figure 13 shows a comparison between the predicted fatigue life (in cycles) for a theoretical DCB model and the FE model of the DCB using the 2D fatigue fracture elements for a cyclic loading between 0 and 40 Newtons.

The theoretical DCB model was:

Given

$$\frac{da}{dN} = C_o \cdot (\Delta G)^{\beta}$$

and for a DCB

$$G \approx \frac{(Pa)^2}{EI\, b}$$

where

$EI$ = is the bending stiffness of one leg

and

$b$ = width

then

$$N = \left(\frac{EIb}{(\Delta P a_o)^2}\right)^{\beta} \cdot \frac{a_o}{C_o(1-2\beta)} \cdot \left[\left(\frac{a}{a_o}\right)^{1-2\beta} - 1\right]$$

The FE model was not actually cycled between the loads *Pmax* and *Pmin*. Instead, the FE model was loaded at a constant load of *Pmax* and the element grew the crack automatically based on the appropriate crack growth calculations. $G_{max}$ was calculated in the element for each crack tip position and $G_{min}$ is estimated from $G_{max}$ based on linear scaling. The FE analysis comparison with theory shows a mesh sensitivity associated with mesh size. The current implementation assumes that $G$ remains constant over the length of the element as the crack extends. For a DCB with a constant force level, the energy release rate, $G$, will increase with crack length. The assumption of constant $G$ results in an over prediction of the number cycles at each element release. The finer mesh effectively mitigates this effect as expected. This element size effect may be

corrected in future versions of the element by taking into account spatially varying energy release rates.

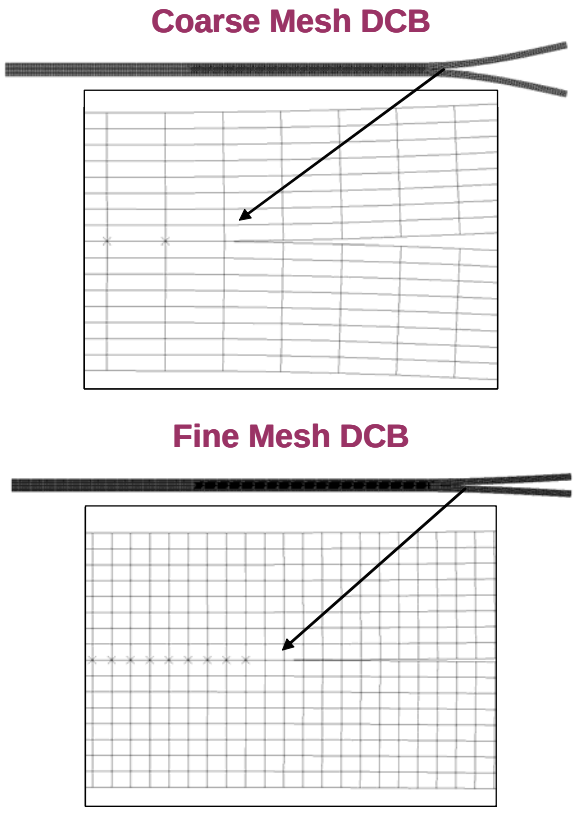


Fig. 11. DCB models for mesh size study of interlaminar fatigue elements

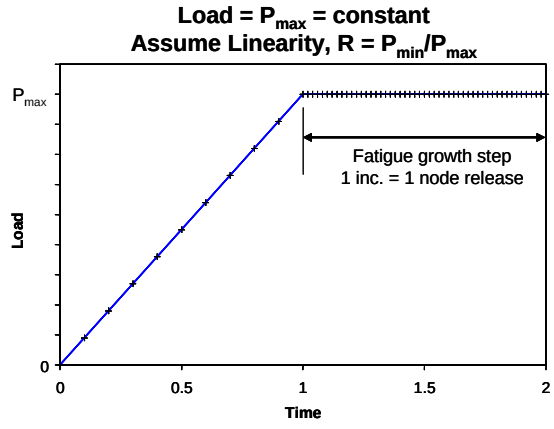


Fig. 12. Load step used for constant loading and assuming linearity

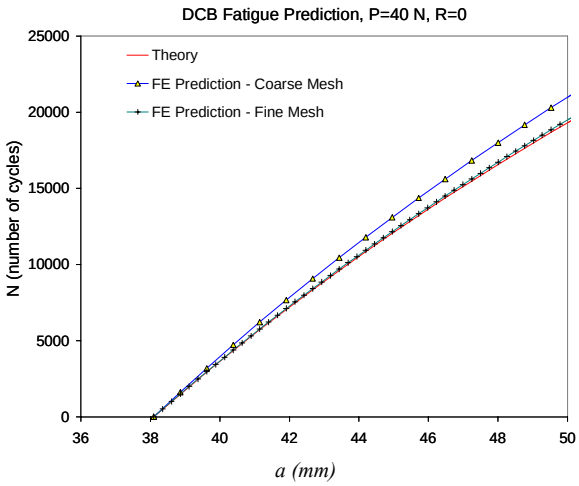


Fig. 13. FE prediction compared to theory

The analysis in its present form may simulate a typical constant load applied to a simple composite structure. However the method will be of limited use for real structure without including the effects on nonlinearity and spectrum loading where nonlinearity has a more significant impact on the analysis. If one assumes linearity, as was done in the DCB demonstration, then the life associated with spectrum loading may be accomplished with the simple load step in Figure 12. An energy release rate, $G$, is calculated at each load block using linear scaling. The manner in which nonlinearity is incorporated in the analysis depends on how much the nonlinearity changes with crack growth. Recall, this analysis is only to represent minimal crack growth. The analysis may be altered so that a nonlinear relationship between load and $G$ may be acquired during the ramp up in Figure 12.

## 5.3 G Onset Approach

A concern expressed in recent NASA publications [12, 13] is that process zone effects (fiber / tow bridging) may influence the Paris law relationship (in a non-conservative manner) when the Paris law is fit to crack growth data, for mode I conditions, measured from DCB fatigue tests. Considering that composite structures are often subjected to a no-growth criterion, NASA recommended simply measuring the energy release rate level required to begin delamination growth when subjected to varying number of fatigue cycles. Such a relationship is expressed as follows.

$$G_{ONSET} = C_1 N^{\alpha} \text{ for } G > G_{thresh}$$

Constants $C_1$ and $\alpha$ are fit to DCB fatigue test data (for mode I conditions), $N$ is the number of cycles to initiate fatigue growth when $G$ equals

$G_{ONSET}$. $G$ must be greater than $G_{thresh}$ to initiate damage. Figure 14 is a plot of the number of cycles to initiate delamination growth at the most critical fatigue element in the model as a function of load level. The load is ramped from zero to the maximum load level and the R-ratio is accounted for in the calculations. An output point is generated at each load increment in the analysis.

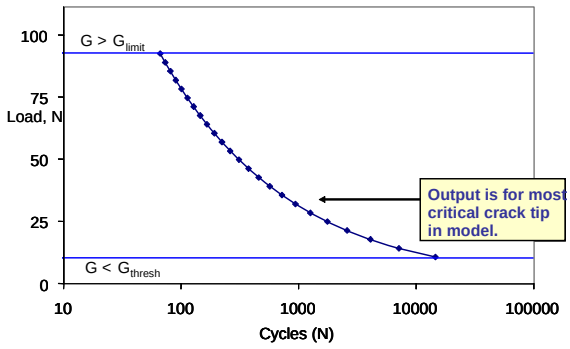


Fig. 14. Predicted DCB fatigue life as a function of load based on $G_{ONSET}$ approach

## 6 Summary

A suite of fracture interface elements have been developed that enable the practical application of the virtual crack closure technique within finite element models along predetermined interfaces. Both 2D (crack tip) and 3D (crack front) implementations have been accomplished for static analysis. A 2D implementation has been accomplished for fatigue analysis. These elements are especially useful if non linear behavior occurs in the model, or if crack propagation predictions are desired. Excellent agreement with test data and other analysis predictions has been shown.

This paper demonstrates the first implementation of a VCCT interface element for performing either fatigue onset analysis or progressive fatigue growth analysis. The key feature of this analysis approach is that energy release rate components are known accurately prior to beginning the element strain softening phase. This capability allows one element or more to be fully released for each time increment and precise accounting of the number of cycles needed to cause fatigue growth over that length. The analyses completed as a part of this study were completely stable and only two iterations (the minimum number) were required to converge at each increment.

Much of the work described in this paper was part of the Composites Affordability Initiative (CAI) program.

The static fracture interface elements described in this paper are contained in US Patent Application 20040148143.

## References

[1] Rybicki, E.F. and Kanninen, M.F. “A Finite Element Calculation of Stress Intensity Factors by a Modified Crack Closure Integral”. *Engineering Fracture Mechanics*, 1977, Vol. 9, pp. 931-938.

[2] Hitchings, D., Robinson, P. and Javidrad, F. “A Finite Element Model for Delamination Propagation in Composites”. *Computers & Structures*, Vol. 60, No. 6, pp.1093-1104. 1996.

[3] Deobald, L.R., Grose, D., Mabson, G.E., Dopker, B. “Design of Robust Bonded Composite Joints Using CAI Pervasive Developed Analysis Tools,” *Defense Manufacturing Conference*, Las Vegas, Nevada, 26 November 2001.

[4] Mabson, G.E. “Fracture Interface Elements”. *Presentation to Mil Handbook 17 Meeting*, Charleston, SC, October 2003.

[5] Mabson, G.E., Deobald, L.R., and Dopker, B. “Fracture Interface Elements”. *Presentation to ASTM Workshop on Computational Fracture Mechanics for Composites*, Salt Lake City, UT, March 2004.

[6] Hoyt, D.M., Mabson, G.E., Deobald, L.R., Dopker, B., Graesser, D.L, Walker, T.H. "Interlaminar Fatigue Analysis Based on CAI Interface Element", *Presentation to ASTM Workshop on Computational Fracture Mechanics for Composites*, Salt Lake City, UT March, 2004.

[7] Engelstad, S.P., Berry, O.T., Renieri, G.D., Deobald, L.R., Mabson, G.E., Dopker, B., Nottorf, E.W., and Clay, S.B. “A High Fidelity Composite Bonded Joint Analysis Validation Study – Part I: Analysis”. *46th AIAA/ASME/ASCE/AHS/ASC Structures, Structural Dynamics, and Materials Conference*, AIAA-2005-2166, 2005.

[8] Deobald, L.R., Mabson, G.E., Dopker, B, Hoyt, D.M., Baylor, J., and Graesser, D.L. “Interlaminar Fatigue Elements for Crack Initiation Onset and Growth Based on Virtual Crack Closure Technique”. *48th AIAA/ASME/ASCE/AHS/ASC Structures, Structural Dynamics, and Materials Conference*, AIAA-2007-2091, Apr. 2007.

[9] Deobald, L.R. et al. “A High Fidelity Composite Bonded Joint Analysis Validation Study – Part II: Analysis Correlation to Test”. *48th AIAA/ASME/ASCE/AHS/ASC Structures, Structural Dynamics, and Materials Conference*, AIAA-2007-2190, Apr. 2007.

[10] Alfano, G., Crisfield, M.A. "Finite Element Interface Models for the Delamination Analysis of Laminated Composites: Mechanical and Computational Issues". *International Journal for Numerical Methods in Engineering*, Vol. 50, 2001, pp. 1701-1736.

[11] *ABAQUS*® is a software product from ABAQUS, Inc., Pawtucket, Rhode Island.

[12] Murri, G.B., O'Brien, T.K. and Rousseau, CQ. "Fatigue Life Methodology for Tapered Composite Flexbeam Laminates". *Journal of the American Helicopter Society*, 1997.

[13] Krueger, R., Paris, I.L., O'Brien, K. *"Fatigue Life Methodology for Bonded Composite Skin/Stringer Configurations"*. NASA/TM-2001-210842, ARL-TR-2432, 2001.

[14] *ASTM D6115-97, "Standard Test Method for Mode I Fatigue Delamination Growth Onset of Unidirectional Fiber Reinforced Polymer Matrix Composites"*. Copyright ASTM International, West Conshohocken, PA, USA, 2004.